

TWO-DIMENSIONAL ELECTRON GAS IN SEMIMAGNETIC SEMICONDUCTOR HgMnTe WITH INVERTED BANDS

V. B. Bogevolnov, I. M. Ivankiv, A. M. Yafyasov

*Institute of Physics, St. Petersburg State University
198904, St. Petersburg, Russia*

*V. F. Radantsev**

*Institute of Physics and Applied Mathematics, Ural State University
620083, Ekaterinburg, Russia*

Submitted 7 June 2000

The two-dimensional electron gas in surface layers on HgMnTe with inverted bands is studied for the first time experimentally and theoretically. It is shown that the structure of the investigated capacitance magnetooscillations in HgMnTe MOS structures is entirely similar to the one in the non-magnetic gapless semiconductor HgCdTe and the sole effect of the exchange interaction is the temperature shift of beat nodes. The information about the exchange parameters is obtained only from modeling the oscillations, because no pronounced changes in the position of oscillations are observed and the separate spin components are not resolved. For the description of the spectrum in the magnetic field, we propose a theory that takes the exchange and spin-orbit interaction into account for materials with direct and inverted bands. The comparison between experiment and theory for different temperatures and exchange interaction parameters is reported. The modeling shows that the spin-orbit splitting by far exceeds the contribution of the exchange interaction. The calculated amplitudes of «partial» oscillations for different spin branches of the spectrum are essentially different in accordance with the difference in the intensities of the corresponding lines in the Fourier spectra of the experimental oscillations.

PACS: 73.20.Dx, 73.40.Qv, 71.70.Ej

1. INTRODUCTION

The peculiar features of, and the interest in, the two-dimensional (2D) electron gas in narrow-gap diluted magnetic (semimagnetic) semiconductors (DMS) are due to two factors. One stems from the $s, p-d$ exchange interaction between band electrons and localized magnetic moments [1]. This interaction changes spin splitting of the band states, which can be varied by external factors, e.g., the magnetic field and temperature. The other factor is due to the peculiarities inherent to small-gap Kane semiconductors, leading to the relativistic-type effects of non-parabolicity, kinetic confinement (motional binding [2]), spin-orbit (SO), splitting, and resonant interband mixing by the surface electric field [3–5]. An important property of 2D electronic systems involving DMS is that both the ex-

change and SO interaction lead to a rearrangement of the spin structure of Landau levels (LLs).

Although historically the first studies of the 2D electron gas in DMS were performed for metal-insulator-semiconductor (MIS) structures based on HgMnTe [6], the experimental results are mostly available for the grain boundaries in HgMnTe and HgCdMnTe with a positive Kane gap $E_g > 100$ meV at the typical Mn content $x = 0.02$ (for higher x , the exchange interaction exhibits itself poorly, which was attributed to the antiferromagnetic interaction between Mn^{2+} ions) [1, 7–9]. This is due to low electron mobility in the previously investigated MIS structures. At the same time, the inversion layers in MIS structures are of particular experimental interest because of the possibility of controlling the depth of the surface quantum well by gate voltage and because of a relative ease and accuracy of the surface potential description (for bicrystals, additional poorly verified assumptions have

*E-mail: victor.radantsev@usu.ru

to be used to describe the self-consistent potential near the grain boundaries [10]). An important point is that these results can be compared with the data for MIS structures based on narrow-gap HgCdTe [4, 11], which is a non-magnetic analogue of narrow-gap DMS.

As to the theoretical description, the subband calculations were carried out only for DMS with direct but not inverted bands and without taking the spinorlike effects into account [1, 6]. However, the SO splitting in asymmetric quantum wells at zero magnetic field (which itself is currently of great interest [4, 5, 12, 14–19]) leads to a rearrangement of the subband magnetic levels. In narrow-gap semiconductors, the magnetic spectrum perturbation is so drastic that the SO interaction cannot be neglected in the theoretical treatment. It must be stressed that as we see in what follows, the SO splitting by far exceeds the exchange interaction contribution, and therefore, it cannot be considered as a correction to the exchange interaction. It is also clear that a treatment based on the semiclassical quantization in the magnetic field of the subband spectrum (calculated in zero magnetic field) is unsuitable for the description of exchange interaction effects. A more rigorous theoretical consideration of the LL structure is required.

In this paper, the peculiarities of 2D electron gas due to the exchange and SO interaction are studied in inversion layers on $\text{Hg}_{1-x}\text{Mn}_x\text{Te}$ with a small Mn content. In Sec. 2, we describe the parameters of the samples and the experimental methods used. The experimental data related to the capacitance oscillations in perpendicular magnetic fields versus gate voltage and magnetic field and their temperature evolution are presented in Sec. 3. The experiments in tilted magnetic fields are discussed in Sec. 4. In Sec. 5, we present the theoretical model based on developing the concept that we proposed previously for non-magnetic Kane semiconductors. In Sec. 6, the results of the computer modeling of capacitance oscillations are presented. The results of comparing the experimental data and theoretical calculations for different temperatures and exchange interaction parameters are discussed.

2. SAMPLES AND EXPERIMENTAL METHODS

MIS structures were fabricated from $p\text{-Hg}_{1-x}\text{Mn}_x\text{Te}$ single crystals. We investigated samples with different values of the Mn content ($x = 0.024, 0.040, 0.060$, and 0.1). The Kane gap E_g and the Kane effective mass m_b (and therefore, x) were

determined independently by the tunnel spectroscopy method for a comparison of band parameters in the bulk with those in the vicinity of the surface. The discrepancy is within the accuracy of the analysis ($\Delta x \sim 0.002 \div 0.003$). Because the tunnel contacts and the studied MIS capacitors were produced using the same technology (see below) and differ only by the insulator thickness, this agreement testifies that the surface layers are chemically close to the bulk. The similarity of the results for the structures with different insulators (fabricated using different methods) supports this conclusion. The fact that the cyclotron masses measured in 2D subbands for small surface concentrations extrapolate to the bulk value m_b is a direct evidence of the absence of a noticeable decomposition in the 2D layer during the structure fabrication process.

At $x < 0.08$, HgMnTe has inverted bands (i.e., becomes semimetal) and traditional galvanometric methods cannot be used because of the shunting of surface conductance by the bulk. We employed the magnetocapacitance spectroscopy method, which is applicable to semiconductors with any sign of the Kane gap. The differential capacitance C of the capacitors and its derivative dC/dV_g with respect to the gate voltage V_g were measured in the dark, typically at 1 MHz and the test signal amplitude 5 mV.

Several methods have been used for forming an insulating film in MIS structures: the anodic oxide formation, the silicon oxide and Al_2O_3 deposition, and the Langmuir—Blodgett film technique. The capacitance magnetooscillations due to the magnetic quantization of the 2D electron gas were observed in all the above structures. The general shapes of the oscillations at the same carrier surface density and the same Mn content are similar. In what follows, we present the results for the structures with a ~ 80 nm thick anodic oxide film. There are several reasons for this choice: (i) the amplitudes of oscillations in these structures are the highest owing to a large insulator capacitance value (this is caused by a large dielectric constant value of the anodic oxide), (ii) the highest surface carrier densities are achieved at low gate voltages $V_g = 10\text{--}15$ V, and (iii) the dielectric constant of the oxide is close to that of a semiconductor, and the contribution of image forces to the surface potential can therefore be neglected in the calculations.

We restrict our consideration to the results for HgMnTe with $x \approx 0.04$ ($E_g = (-100 \pm 5)$ meV). The amplitudes of the oscillations for other samples are much less even at 4.2 K and rapidly decrease with increasing the temperature. (For $x \approx 0.024$, this is

caused by a small cyclotron energy due to a large Kane gap; for $x \approx 0.06$ and $x \approx 0.1$, this is the result of a large doping level of available materials.) As a result, we could not obtain reasonably accurate information about the oscillation temperature evolution where the specificity of DMS is manifested. As to the measurements at $T = 4.2$ K, the subband parameters extracted from oscillations for these samples are similar to those for HgCdTe with the same band parameters and agree well with the theory.

On the other hand, the samples with $x = 0.04$ are best suited to the purpose of this first study aimed at investigating the peculiarities of the 2D electron gas in DMS with inverted bands, where (i) the SO and exchange interaction effects are expected to be more clearly pronounced and (ii) the results can be compared with those for well studied surface layers on gapless HgCdTe with $E_g \sim -(50-100)$ meV [4, 20]. For a small gap $|E_g| < 100$ meV, the parameters of 2D subbands depend only weakly on E_g (except in the case of small subband occupancies) [4, 20]. By contrast, the subband parameters are more sensitive to the doping level. For this reason, we present the results for two samples with $N_A - N_D = 1.2 \cdot 10^{16}$ cm $^{-3}$ (sample S1) and $N_A - N_D = 1.5 \cdot 10^{17}$ cm $^{-3}$ (sample S2 with the gate area $S = 7.7 \cdot 10^{-4}$ cm 2 and the insulator capacitance $C_{ox} = 155.1$ pF).

3. MAGNETOCAPACITANCE IN PERPENDICULAR MAGNETIC FIELDS

Figure 1 shows the capacitance–voltage characteristics at $T = 4.2$ K in the magnetic field $B = 4.5$ T perpendicular to the 2D layer for the sample S2. The $C(V_g)$ characteristics are typical for the low-frequency behavior. This means that 2D electrons in the inversion layers contribute predominantly to the measured capacitance under the inversion band bending. The low-frequency conditions with respect to the minority carriers are satisfied in all the investigated frequency range 30 kHz–5 MHz. The wide hysteresis loop and the dependence of the $C(V_g)$ characteristics on the voltage sweep rate are observed. At a fixed V_g , the capacitance changes in time because of a flat-band voltage shift ΔV_{fb} . The time constant is of the order of several minutes and is almost independent of the temperature. This behavior points to the charge tunnel exchange between the semiconductor and the slow traps in the insulator. The history dependence and instability are manifested in all the investigated HgMnTe-based MIS structures. This is in contrast with the HgCdTe- and

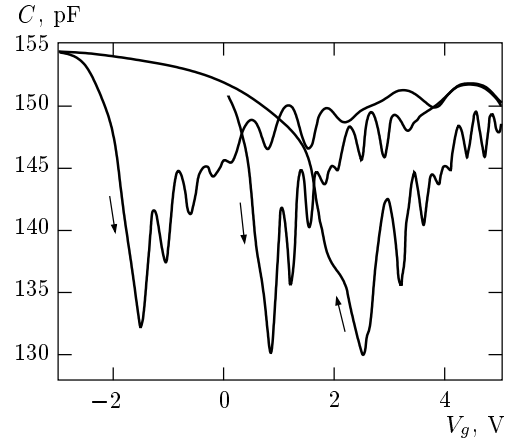


Fig. 1. Capacitance–voltage dependences in the magnetic field $B = 4.5$ T perpendicular to the 2D plane for sample S2 at different gate voltage sweeps. The arrows indicate the sweep direction. The sweep rate is 2 V/mn

HgTe-based structures with the same insulators that we investigated simultaneously.

The voltage dependence of the charge density $eN_s(V_g)$ induced in the inversion layer is sublinear. This is demonstrated by the non-equidistance of quantum oscillations of the capacitance $C(V_g)$ (see Fig. 1). The tunneling of electrons from the 2D layer into the oxide causes a saturation of the $N_s(V_g)$ dependence at $V_g - V_{fb} \approx (10-15)$ V. As a result, the N_s range accessible for investigations is limited by the value $(3-4) \cdot 10^{12}$ cm $^{-2}$ (in HgCdTe, the N_s values up to 10^{13} cm $^{-2}$ can be obtained). Although the hysteresis effects hamper the measurements, the discussed physical results are not affected by the band bending instability. This instability is caused by the transient processes but not by degradation. Although the $C(V_g)$ characteristics are history dependent, they are completely repeatable if the voltage range, rate, and direction of the sweep are the same. To assure the stability of the band bending during the measurement of $C(B)$ oscillations, the sample was held at a given voltage for 5–15 minutes. The identity of $C(B)$ plots registered at increasing and decreasing the magnetic field (i.e., at different times) was examined for each $C(B)$ curve. When the temperature (or angle) dependences of the $C(B)$ oscillations were measured, the long term stability was checked by the repetitive measurement of the initial $C(B)$ plot (for a given measurement cycle).

The $C(B)$ oscillations (and consequently, the subband occupancy and the surface potential) measured at the same capacitance magnitude in zero magnetic

field $C(0)$ are identical, irrespective of the voltage (the value of the latter for any given $C(0)$ is determined by the flat-band voltage, which is history- and time-dependent). When the dc gate voltage (or the flat-band voltage at the same V_g) is changed, the filling of interface states is also changed but does not respond to the ac ripple, i.e., the interface states do not contribute to the capacitance. This occurs for all frequencies and temperatures and testifies that the high-frequency conditions with respect to interface states are satisfied. Thus, there is a «one-to-one correspondence» between $C(0)$, the band bending, and the surface density of 2D electrons $N_s = \sum N_i$ (where i is the 2D subband number).

The subband parameters are presented below as functions of N_s . Contrary to the dependence on V_g , their dependence on N_s is not affected by the hysteresis effects or any specific parameters of MOS capacitors; the same N_s dependence is common to a given HgMnTe sample. It may be noted that there are some positive aspects of hysteresis. We have the possibility to investigate the 2D electron gas in the same surface quantum well on the same sample but with a different interface charge. This is important, in particular, in the investigation of scattering mechanisms.

Typical $C(B)$ oscillations are presented in Fig. 2 together with their $1/B$ Fourier transforms. The individual spin components have not been observed in the oscillations at any N_s even for the lowest LLs. On the other hand, the oscillation beats and the Fourier spectra distinctly demonstrate the presence of two frequencies connected with the SO splitting of each 2D subband. The surface densities in the spin-split subbands N_i^+ and N_i^- determined from Fourier transforms are plotted in Fig. 3. The carrier distribution among 2D subbands is different for the two samples. The concentrations N_s corresponding to the «starts» of the excited subbands increase as the doping level increases and agree well with the theoretical calculations in which the bulk values of $N_A - N_D$ are used. This fact also testifies that the disruption of stoichiometry in surface layers that could be caused by the migration of atoms is insignificant. A discrepancy with the theory is detectable only in the relative differences of occupancies $\Delta N_i/N_i = (N_i^- - N_i^+)/(N_i^- + N_i^+)$ in the small N_s range. Similar disagreement also occurs for inversion layers on HgCdTe. Possible reasons for this behavior are discussed in Ref. [4]. The intensities of Fourier lines for the high-energy branch I_i^+ and the low-energy branch I_i^- are different and the ratio I_i^-/I_i^+ decreases with increasing N_s .

The structure of oscillations and the subband pa-

rameters extracted from oscillations are identical to those in HgCdTe. No features due to the exchange interaction are manifested. Because the exchange effects are determined by the magnetization and can be varied by the temperature, the investigation of the temperature evolution of oscillations is of primary interest. The results for sample *S2* are shown in Fig. 2. As can be seen, no pronounced changes in the position oscillations are observed. The shift of beat nodes to higher gate voltages and to lower magnetic fields (to larger LL numbers) with increasing the temperature (and hence, with decreasing the magnetization) is the sole temperature effect, besides the usual decrease of oscillation amplitudes. This shift must be attributed to the features inherent to semimagnetic semiconductors because neither the positions of oscillations nor those of the beat nodes change with the temperature in HgCdTe-based structures.

4. MEASUREMENTS IN TILTED MAGNETIC FIELDS

Although there is no doubt that we are dealing with a 2D system (the existence of the magnetooscillation effect in the capacitance and the observation of magnetooscillations versus gate voltage already testify to it), the experiments in a tilted magnetic field were also performed. Some results for sample *S2* are presented in Fig. 4. The magnetic field positions of the oscillation extrema and the fundamental fields in the Fourier spectra (to a smaller extent) vary only roughly as the cosine of the angle θ between \mathbf{B} and the normal to the 2D layer. Clearly distinguishable deviations from this behavior are observed. Namely, the experimental angle dependences are stronger.

There are several reasons for this deviation from the classical cosine dependence, because a number of physical factors are ignored in the simplified model [21]. First, in the strictest sense, this behavior, even for the parabolic dispersion, is valid only for an ideal 2D system. The condition to be satisfied for the cosine dependence is $\langle r \rangle / \langle z \rangle \gg 1$, where $\langle r \rangle$ and $\langle z \rangle$ are the respective mean sizes of the wave function in the 2D plane and in the confinement direction. For narrow-gap semiconductors, the width of the surface quantum well is relatively large and such a strong requirement may be not fulfilled (we also note that $\langle z \rangle$ is energy dependent in this case). In a strong magnetic field and at a small surface concentration, the cyclotron radius and the 2D layer width can be comparably-sized (especially, for excited subbands) and the diamagnetic shift

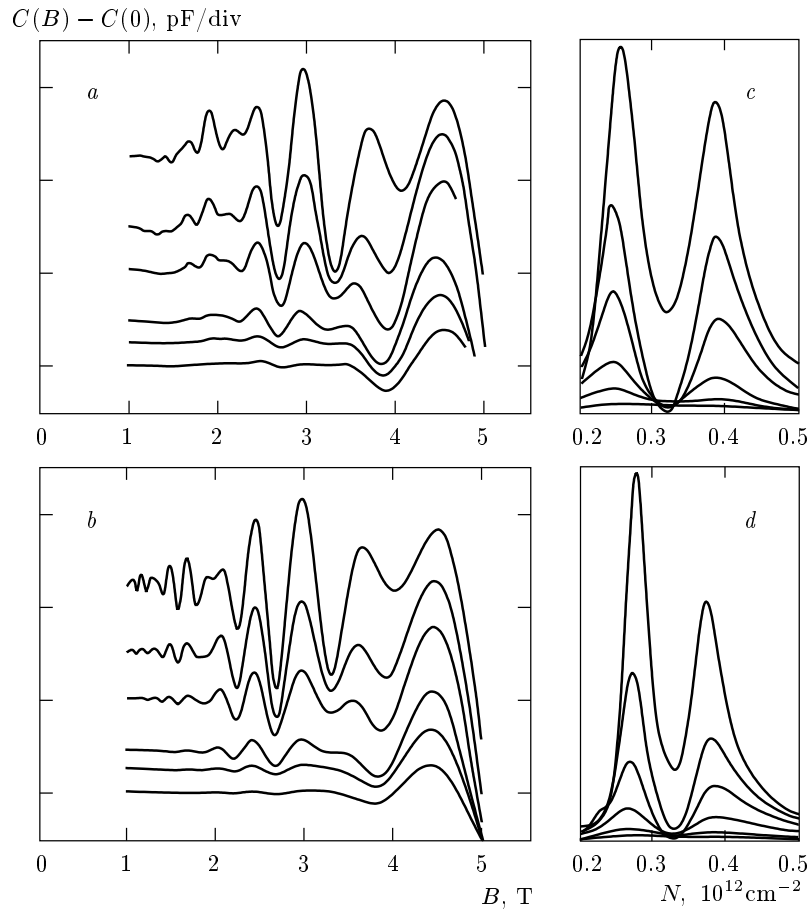


Fig. 2. Experimental (a) and simulated (b) temperature evolutions of $C(B)$ oscillations and their Fourier spectra (c, d) for sample $S2$. Temperature (from top to bottom): 4.2, 10, 15, 22, 29 K, and 35 K. The values $T_D = 11$ K for $i = 0$, $T_D = 9.5$ K for $i = 1$, and $T_N = 10$ K are used in the calculation

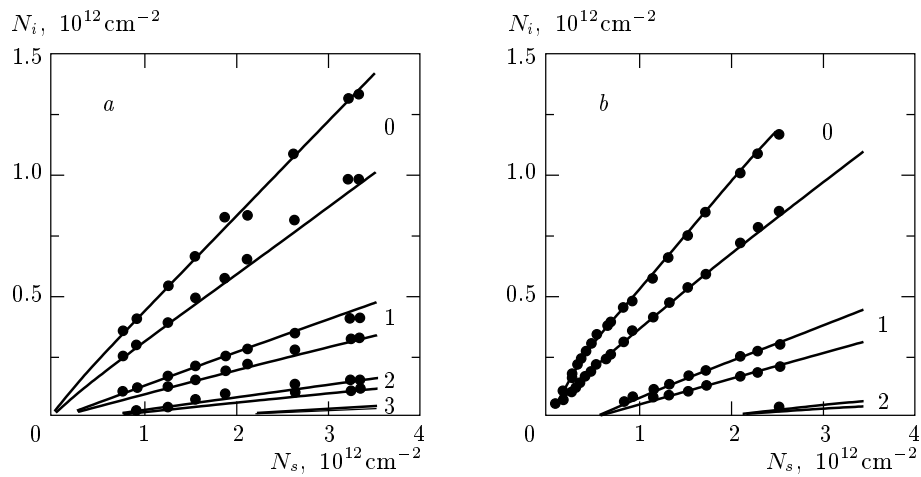


Fig. 3. The calculated (lines) and measured (points) distributions of 2D electrons among the spin-split subbands for $S1$ (a) and $S2$ (b) samples. The theoretical dependences are calculated as in Ref. [4]. The numbers at lines are the subband numbers

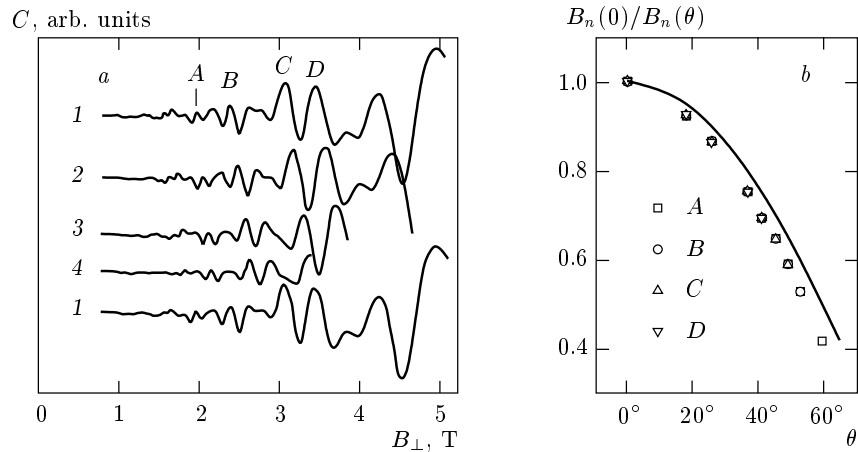


Fig. 4. (a) Capacitance oscillations plotted versus the normal component B_{\perp} of the applied magnetic field for sample $S2$ at $N_s = 1.62 \cdot 10^{12} \text{ cm}^{-2}$. The angle θ between \mathbf{B} and the normal to the $2D$ layer: 1 — 0° ; 2 — 26° ; 3 — 42° ; 4 — 50° . To demonstrate the reproducibility of the results, we plotted two $C(B_{\perp})$ oscillations for $\theta = 0$. The upper and lower plots are measured before and after the angle dependence measurements respectively. (b) The angle dependences $B_n(0)/B_n(\theta)$ for oscillation maxima marked on the upper $C(B)$ plot. The line is the cosine function

must weaken the angle dependence. This is contrary to the experimental behavior. Second, the cosine relation is obtained for spinless particles. This is not the case in a real system. Third, the SO interaction is neglected in this simple consideration. Undoubtedly, spinlike effects can affect the spectrum in a tilted magnetic field and modify the angle dependence.

Finally, the exchange interaction can also give an additional contribution to the deviation from the simple angle dependence. This assumption has experimental support. For comparison, we investigated the HgCdTe-based samples in a tilted magnetic field. Under the same conditions, they also manifest a deviation from the cosine behavior. However, the deviation is weaker than for gapless HgMnTe and has the opposite sign. At the same time, the samples based on HgCdTe with $E_g > 0$ show a deviation of the same sign as in HgMnTe, but smaller in magnitude. Contrary to HgCdTe samples, changes in the structure of oscillations are observed in HgMnTe inversion layers. Namely, the beat nodes in oscillations $C(B_{\perp})$ (with $B_{\perp} = B \cos \theta$) are shifted to the lower LL numbers with the increase of θ (i.e., with the increase of the total magnetic field B), see Fig 4. We note that the direction of the shift occurring with the increase of B (with B_{\perp} kept fixed) is similar to the one observed with decreasing the temperature.

These experimental observations testify that the behavior in tilted magnetic fields is markedly affected by both the SO interaction (which essentially depends on

the E_g sign [4]) and the exchange interaction. For narrow-gap semiconductors, the theoretical analysis requires a consideration of spin from the outset. Strong SO and exchange interactions and the resonant effects lead to a serious complication of the theoretical description even for the perpendicular orientation. The calculations in tilted magnetic fields are troublesome even for the simplest parabolic Hamiltonian with a k -linear Rashba term. At present, we cannot make a reasonable theoretical analysis of the effects in tilted fields and we restrict our analysis to the case of the perpendicular orientation.

As shown in Sec. 3, the analysis based on the Fourier transform of oscillations for different temperatures cannot yield any information about the exchange interaction. On the other hand, these data cannot be obtained from spin splitting either because, as noted above, the separate spin components are not observed in the oscillations at any temperatures. Thus, we must settle the question by the capacitance magnetooscillations modeling.

5. THEORETICAL ANALYSIS

To simulate the capacitance magnetooscillations, the density of states (DOS) must be calculated as a function of B (or V_g). This requires knowing the subband spectrum in the magnetic field and the broadening of the Landau levels. Under the homogeneous

magnetic field $\mathbf{B}(0, 0, B)$ parallel to the confinement direction (the surface potential $V = V(z)$), the motion in the 2D plane can be quantized using the mean

field approximation for the exchange interaction. In the framework of a six-band Kane model, the subband LL energy $E_n(B)$ is determined by the matrix equation

$$\begin{bmatrix} -E_- + \alpha & \frac{E_B \sqrt{3(n-1)}}{2} & \frac{E_B \sqrt{n}}{2} & 0 & 0 & s_b \hbar k_z \\ \frac{E_B \sqrt{3(n-1)}}{2} & -E_+ + 3\beta & 0 & 0 & 0 & 0 \\ \frac{E_B \sqrt{n}}{2} & 0 & -E_+ - \beta & s_b \hbar k_z & 0 & 0 \\ 0 & 0 & s_b \hbar k_z & -E_- - \alpha & \frac{E_B \sqrt{3(n+1)}}{2} & -\frac{E_B \sqrt{n}}{2} \\ 0 & 0 & 0 & \frac{E_B \sqrt{3(n+1)}}{2} & -E_+ - 3\beta & 0 \\ s_b \hbar k_z & 0 & 0 & -\frac{E_B \sqrt{n}}{2} & 0 & -E_+ + \beta \end{bmatrix} \begin{pmatrix} f_1^{n-1}(z) \\ f_3^{n-2}(z) \\ f_5^n(z) \\ f_2^n(z) \\ f_4^{n-1}(z) \\ f_6^{n-1}(z) \end{pmatrix} = 0, \quad (1)$$

where $E_{\pm}(z) = E_n - V(z) \pm E_g/2$, $s_b = \sqrt{|E_g|/2m_b}$ is the Kane velocity, n is the LL number, and $E_B = \sqrt{2m_b s_b^2 \hbar \omega_b} = \sqrt{2} s_b \hbar / \lambda$ (with $\hbar \omega_b = \hbar e B / m_b c$ being the cyclotron energy and $\lambda = \sqrt{c \hbar / e B}$ the magnetic length). We denote $\alpha = x N \alpha' \langle S_z \rangle / 2$ and $\beta = x N \beta' \langle S_z \rangle / 6$, where x is the MnTe mole fraction, N is the number of unit cells per unit volume, and α' and β' are the respective exchange integrals for the Γ_6 and Γ_8 bands. The thermodynamic average $\langle S_z \rangle$ of the z -component of a localized spin S (with $S = 5/2$ for Mn^{2+} ions) defines the magnetic field and temperature dependence of the exchange effects and can be described via the normalized Brillouin function $B_S(x)$,

$$\langle S_z \rangle = -S(1-x)^{18} B_S \left(\frac{2\mu_B B}{k_B(T+T_N)} \right), \quad (2)$$

where T_N is the effective temperature arising from the antiferromagnetic interaction between Mn^{2+} ions [22, 23].

To solve Eq. (1), we use the concept proposed by Zel'dovich and Migdal [24, 25] for the related problem of describing the vacuum condensate of Dirac electrons near supercritical nuclei; we have used this model for the Kane Hamiltonian [4, 26]. In this scenario, the problem is reduced to a Schrödinger-type equation with the effective potential in which the terms responsible for non-parabolicity, spin-orbit splitting, and the «resonant» shift are easily singled out. The qualitative similarity and the quantitative difference between the cases where $E_g > 0$ and $E_g < 0$ are also clearly seen. As in Ref. [4], we use the semiclassical approximation both

for the calculation of the surface potential $V(z)$ and for the quantization of the resulting equations. The validity of this approach in narrow-gap semiconductors was argued and demonstrated by comparing with numerical self-consistent calculations in many papers (see Ref. [4] and references therein). The simplicity of the method is of considerable advantage for the purposes of oscillations modeling.

Arguing as in Ref. [26], we obtain from (1) the semiclassical expression for the «spin-split» z -components of the wave vector

$$k_z^{\pm} = \frac{\sqrt{2m_b s_b^2}}{s_b \hbar} \{ K \mp [K^2 - (E_{eff} - U^+)(E_{eff} - U^-) + U_{so}^+ U_{so}^-]^{1/2} \}^{1/2}, \quad (3)$$

where

$$K = E_{eff} - (U^+ + U^-) / 2 - m_b s_b^2 C_g^2 (R_n^+ - 1)(R_n^- - 1)$$

and the effective energy is $E_{eff} = (E^2 - m_b^2 s_b^4) / 2m_b s_b^2$. In the effective potential $U^{\pm} = U_0 + U_B^{\pm} + U_{exc}^{\pm} + U_R^{\pm}$, we single out the «Klein–Gordon» term

$$U_0 = (V^2 - 2EV) / 2m_b s_b^2,$$

two spin-like terms, namely the «magnetic potential»

$$U_B^{\pm} = E_B^2 [g^2 n R^{\pm} + 3(n \pm 1)(E_+ \pm \beta) / (E_+ \pm 3\beta)] / 2m_b s_b^2$$

and the «exchange potential»

$$U_{ex}^{\pm} = [\alpha\beta \pm (\alpha E_+ + \beta E_-)] / 2m_b s_b^2,$$

and the «resonant» term describing a «spin–interband» interaction arising from the mixing of the Γ_6 and Γ_8 bands by the electric field,

$$U_R^\pm = \frac{s_b^2 \hbar^2}{2m_b s_b^2} \left[\frac{3}{4} \left(\frac{1 + L_n^\pm}{H_n^\pm} \right)^2 + \frac{L_n^\pm}{H_n^\pm (E_+ \pm 3\beta)} \right] \times \\ \times \left(\frac{dV}{dz} \right)^2 + \frac{s_b^2 \hbar^2}{4m_b s_b^2} \frac{(1 + L_n^\pm)}{H_n^\pm} \frac{d^2 V}{dz^2}.$$

The spin-orbit term involved in Eq. (3) is

$$U_{so}^\pm = C_g s_b \hbar \sqrt{R_n^\mp} \left[\frac{1 + L_n^\pm}{H_n^\pm} + \frac{1 + L_n^\mp}{2H_n^\mp} (R_n^\pm - 1) \right] \frac{dV}{dz}.$$

In the above expressions, we used the notations

$$R_n^\pm = H_n^\pm / H_n^\mp, \quad C_g^\pm = C_g \sqrt{R_n^\mp} (R_n^\pm - 1),$$

and

$$C_g = g E_B \sqrt{n} / 4m_b s_b^2.$$

We must put

$$L_n^\pm = 3E_B^2 (n \pm 1) / 4(E_+ \pm 3\beta)^2,$$

$$H_n^\pm = E_- \pm \alpha - L_n^\pm (E_+ \pm 3\beta),$$

and $g = -1$ for surface electrons in Kane semiconductors with $E_g < 0$, and $L_n^\pm = 0$, $H_n^\pm = E_+ \pm \beta$, and $g = +1$ in semiconductors with $E_g > 0$. Together with the Bohr–Sommerfeld quantization rule, Eq. (3) defines the magnetic levels $E_n^\pm(i, B)$ in the surface quantum well $V(z)$. It must be stressed that the exchange interaction causes not only the appearance of an exchange term in the effective potential, but also a modification of the terms describing the «resonant» and SO interaction.

The calculations show that the SO splitting by far exceeds the contribution of the exchange interaction. Furthermore, the SO interaction also suppresses the splitting due to the exchange interaction. As an example, the SO splitting near the Fermi level corresponding to the first beat node in Fig. 2 is 17.2 meV (at the subband Fermi energy $E_{F0} = 78$ meV). If we take the exchange interaction into account, the splitting increases by only 4.2 meV even at $T = 4.2$ K. At the same time, the exchange splitting calculated without taking the SO interaction into account is 5.6 meV. This is why the exchange effects manifest themselves only as a small change in the structure of oscillations near the beat nodes, where the oscillations from different spin branches quench each other.

The SO interaction leads to such a drastic reconstruction of the 2D spectrum in magnetic fields that the

description of the spin splitting by the non-relativistic g -factor parameter loses its physical meaning. This is also true for narrow-gap DMS with $E_g > 0$. In view of this effect, the results of the analysis of 2D systems in asymmetric quantum wells in these materials are to be revised, because they ignore the SO interaction.

6. RESULTS OF MODELING AND DISCUSSION

In calculating the differential capacitance of the space charge region, the density of states in the magnetic field was described neglecting the mixing between LLs and assuming a Gaussian shape of each level, as we did in Ref. [26]. The surface potential and the subband Fermi energies are assumed to be constant when the magnetic field is changing. The alternative model is based on the assumption that the surface density is fixed. However, both models give indistinguishable results for a sufficiently large LL broadening (this is manifested by the cosine form of experimental oscillations) [27]. The temperature dependences of band parameters and the bulk Fermi energy are accounted for in the calculations.

Although we performed the calculations for a different set of exchange parameters (literature data vary markedly, see Refs. [1, 28–30] and references therein), the results discussed in this Section correspond to $N\beta' = 1.5$ eV and $N\alpha' = -0.4$ eV, unless otherwise specified. These values are close to those obtained in Refs. [28, 29] by the tunnel spectroscopy method for narrow-gap and gapless HgMnTe with small $|E_g|$. We suppose that these data (with similar values for gapless HgMnTe obtained in many works, see references in [1, 28, 29]) are more suitable for the purposes of this work, because the typical electron energies are of the order of or even considerably larger than $|E_g|$ in the studied surface quantum wells. In tunnel experiments, the LL energy positions of « p -electrons» as functions of the magnetic field are measured at energies up to 150 meV.

Once the exchange parameters are chosen, two parameters can be obtained when the modeling fits the experimental data: the effective temperature T_N , which describes the temperature shift of beat nodes, and the Dingle temperature, which determines the oscillation amplitudes (and which we use as a characteristic of the scattering).

In calculations, we assume that T_D is the same for both spin-orbit branches. This assumption is supported experimentally. When three or more beat nodes

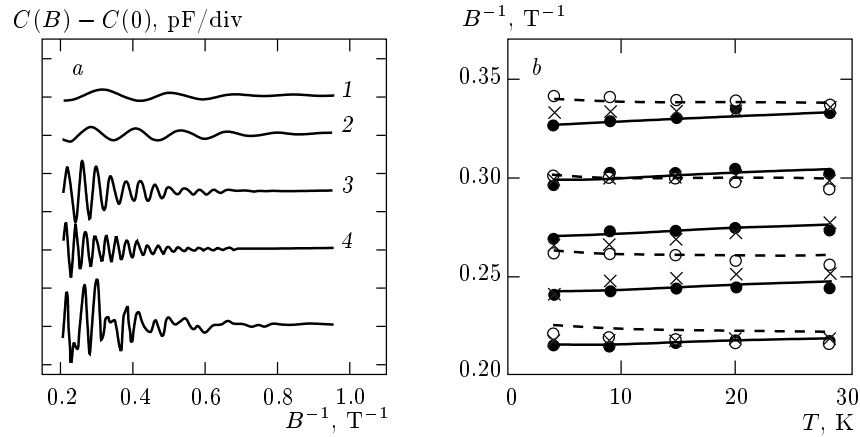


Fig. 5. (a) «Partial» oscillations for different spin sub-subbands i^\pm (curve 1 — 1^+ ; 2 — 1^- ; 3 — 0^+ ; 4 — 0^-) extracted from the experimental $C(B)$ trace (the lower plot). (b) Magnetic field positions of (i) the maxima of experimental oscillations (crosses), (ii) «partial» oscillations maxima extracted from the experimental $C(B)$ traces (circles) and (iii) LLs calculated at the Fermi energy (lines) for the ground subband $i = 0$ as functions of temperature. Solid lines and solid circles correspond to the low-energy spin branch (0^-), the dashed line and open circles to the high-energy branch (0^+)

are observed in the oscillations, the «partial» oscillations related to different spin branches can be extracted from the experimental $C(B)$ traces using the Fourier filtration and the inverse Fourier transform (see Fig. 5a). The T_D values determined from fitting of «partial» oscillations turn out to be close for both branches within the accuracy of the analysis.

At the same time, the amplitudes corresponding to these branches can differ considerably (up to several times). This difference is not surprising. Although DOS is higher at $B = 0$ in the low-energy branch, the corresponding amplitudes can be smaller (even if the relaxation times are equal), because the lower cyclotron energy in this branch leads to a smaller amplitude factor. The calculated amplitude ratio A_c^-/A_c^+ decreases rapidly as N_i increases. This behavior correlates well with the decreasing ratio of the Fourier line intensities observed experimentally. The difference of the amplitudes for different spin components of oscillations mentioned in Refs. [11, 14] are therefore expected to be different for 2D systems with a strong SO interaction without invoking the spin-dependent scattering.

Although the general shapes of the simulated and measured oscillations $C(B)$ are well matched, the exact magnetic field positions of the peaks and beat nodes are somewhat different. This is because a number of physical factors are ignored or cannot be exactly taken into account in the theory (the contribution of remote bands, the interface contribution to the SO interaction (see below), the deviation of the real surface potential and the Landau level shape from the calculated ones,

etc.). The adjustable phase correction was introduced for convenience for the comparison of the temperature evolution in the measured and calculated oscillations. Its magnitude was chosen to fit the high-field node position of the beat pattern at $T = 4.2$ K. None of the physically meaningful results that we discuss are affected by the choice of this factor.

The oscillations calculated with this correction and their Fourier transforms are plotted in Fig. 2. The agreement is quite good with respect to the structure of oscillations and the amplitudes. However, a distinguishable difference in the «number» of oscillations between beat nodes for the measured and calculated plots is observed. These results, as well as similar data on the $dC/dV_g(V_g)$ oscillations, testify to a small (but distinguishable) underestimation of the SO splitting by the theory. (We note that in the high- N_s range, the analysis based on the Fourier spectra does not give a clearly detectable discrepancy between experiment and theory.) This inconsistency with the theory can be caused by the interface contribution to the SO splitting [16], which cannot be treated in the framework of the effective mass method.

According to the experiment, the individual spin components are not exhibited in simulated $C(B)$ or $dC/dV_g(V_g)$ oscillations even for the lowest LLs at any reasonable broadening parameters, magnetic fields of experimental interest, and temperatures. A decrease of magnetization with increasing temperature results in a slight energy shift of the calculated spin sublevels. However, the position of the resulting oscilla-

tions on the magnetic field is almost unchanged (see Fig. 5b), except for the oscillations near the beat nodes (as occurs experimentally). The calculated rate of the temperature shift of beat nodes with the temperature depends on N_i and the node number. At the same time, the value of T_N extracted from the fit of the temperature evolution of the oscillations is almost the same for different nodes and different N_i . The simulation results are not critically dependent on the exact value of T_N chosen. However, the «best fitting» value $T_N = (10 \pm 1.5)$ K must be a reasonably good estimate.

Unfortunately, as far as we know, the low-temperature data on the T_N value for bulk HgMnTe with $x = 0.04$ are absent. Most of the literature data are obtained either for high temperatures or for samples with the Mn content $x \leq 0.025$. However, the value $T_N = 10$ K does not contradict other published data. If the sample-independence of the spin–spin interaction is postulated, T_N is nearly proportional to $x(1-x)^{18}$ [22]. Using the low-temperature data in Ref. [22] for a sample with $x = 0.01$ ($T_N = 2.9$ K at $T = 2$ K), we can estimate the value of T_N for samples with $x = 0.04$ as $T_N \approx 8$ K. This is somewhat less than the measured value, but T_N can also be temperature dependent [33]. For example, for the same sample with $x = 0.01$, T_N is equal to 7 K in the high-temperature range [22]. It must be noted that the above estimates are based on assumptions (including the phenomenological expression itself, Eq. (2)) that can be violated for $x > 0.02$ and for low temperatures.

We now turn to the dependence of the observed exchange effects on the value of the exchange parameters. As mentioned above, the exchange interaction is very weakly manifested in the studied system, showing itself as only a slight temperature shift of beat nodes. Because the oscillation amplitudes are small in the neighborhood of nodes even at $T = 4.2$ K and because they decrease drastically with the temperature, the narrow range of $T < 10$ –15 K is accessible to the quantitative analysis. Thus, the results are not critically sensitive to the choice of $N\beta'$ and $N\alpha'$. Because the shift rate depends on the product of the exchange parameters $N\beta'$ and $N\alpha'$ and the magnetization $\langle S_z \rangle$, the variations in $N\beta'$ and $N\alpha'$ can be cancelled by the variation in T_N , which is used as an adjustable parameter.

Only the shift of beat nodes to low LL numbers is observed at low temperatures with decreasing $N\beta'$ (the shift is slightly sensitive to the variations of $N\alpha'$ in the $-(0.25$ – $0.5)$ eV range). As a result, the rate of the temperature shift of nodes decreases and becomes less than the one calculated at $N\beta' = 1.5$ eV. However, at $N\beta' > 0.75$ eV, this decrease can be cancelled by a

decrease in T_N . For $N\beta' = 1.0$ eV and $N\alpha' = -0.4$ eV, the shifts coincide with those found for $N\beta' = 1.5$ eV and $N\alpha' = -0.4$ eV if the value $T_N = 4$ K is chosen. In both cases, the oscillations are practically the same at all B (including the ranges near the beat nodes) and T . However, the value $T_N = 4$ K seems to be too small for $x = 0.04$.

At the same time, the experimental results cannot be described at $N\beta' < 0.7$ eV. The measured shift rate is nearly twice as large as that calculated at $N\beta' = 0.6$ eV and $N\alpha' = -0.4$ eV (the values given in Ref. [30]) even if $T_N = 0$ is chosen. Although the exchange effects in the studied systems with a strong interband mixing are suppressed by the SO splitting, this discrepancy is beyond the limits of experimental error. It is easy to verify that the experimental data (the energy position of LLs and its temperature shift) presented in Refs. [28, 29] for bulk HgMnTe with small $|E_g|$ also cannot be explained at $N\beta' < 1.0$ – 1.2 eV even for $T_N = 0$. As already noted, the value of $N\beta'$ reported in works on gapless HgMnTe falls typically within 0.9–1.6 eV.

The terms in Eq. (3) containing the parameter β play the dominant role at the conditions corresponding to a typical experimental situation. On the other hand, the results are only slightly sensitive to reasonable variations of α even in the inversion layers on HgMnTe with $E_g > 0$. It must be stressed that at the energies $E \sim |E_g|$ or higher, the terms involving β must also give the leading contribution in the bulk of DMS with $E_g > 0$. As a rule, however, the electrons with the energy near the band bottom are tested in the investigation of bulk properties. At the same time, in the surface quantum wells on narrow-gap semiconductors, the typical electron energies are of the order of or even considerably larger than $|E_g|$. In this work, the band bending ranges up to 450 meV (this value corresponds to $N_s \approx 4 \cdot 10^{12}$ cm $^{-2}$). The above analyses of the experimental data revealed that the bulk values of the exchange coupling constants obtained at low-energy experiments are workable even at these high energies.

As a related issue, we note that the decrease of $|N\alpha'|$ in a wide-gap CdMnTe–CdMgMnTe quantum well with the increase of energy is reported in a recent paper [31]. The effect is attributed to the admixing of Γ_8 band states to the Γ_6 band at finite \mathbf{k} -vectors, which leads to switching on a kinetic exchange of the Γ_6 band electrons with the d electrons of Mn ions. We note that in narrow-gap semiconductors, the interband mixing described by Kane Hamiltonian (1) results in a strong (and energy dependent) contribution of the $N\beta'$ containing terms to the spectrum of the Γ_6 band. This

is true without taking the energy dependence of the $N\alpha'$ parameter into account. As for the Γ_8 band electrons, the value of the exchange parameter $N\beta'$ is from the outset governed mainly by the kinetic exchange (at any \mathbf{k} -vector). In this case, an increase of the \mathbf{k} -vector cannot play a critical role. The absence of an essential change in the value of $N\beta'$ is noted in Refs. [31, 32].

The Dingle temperatures T_D determined from the fitting are close to those in HgCdTe-based structures. In the high- N_s range, the T_D values are dictated by the surface roughness scattering. The best agreement between the experimental and calculated values of T_D is achieved at the correlation length $\Lambda \approx (110\text{--}120)$ Å and at the average interface displacement $\Delta \approx (20\text{--}25)$ Å. Using the T_D values, we can estimate the electron mobility as $0.8 \cdot 10^4$ cm²/V·s in the $i = 0$ subband and $1.5 \cdot 10^4$ cm²/V·s in the $i = 1$ subband for sample *S1* at $N_s \sim 10^{12}$ cm⁻², which is close to the value $1 \cdot 10^4$ cm²/V·s measured for grain boundaries in p-HgMnTe [7].

As in HgCdTe [26], somewhat larger values of T_D are detected at small surface densities $N_s < 5 \cdot 10^{11}$ cm⁻². According to Ref. [26], theoretical estimates show that no increase in T_D with the decrease of N_s within this range can be caused by the Coulomb scattering from chargers in the oxide. This conclusion has direct experimental evidence in the present work. It can be seen in Fig. 1 that the charges localized in the oxide differ by a factor of several times for different sweep cycles. If the Coulomb scattering were important, the amplitudes of oscillations corresponding to different cycles (different V_{fb}) but with the same N_s (the same LL number at a fixed magnetic field) would be different. However, the oscillation amplitudes are the same. A possible cause for the increase of the LL broadening at small N_i is the intersubband scattering [34].

This work was supported by the European Commission Esprit project № 28890 NTCONGS EC, by Award № REC-005 of U. S. Civillian Research & Development Foundation (CRDF) and by the Grant from Education Committee of Russia.

REFERENCES

1. J. K. Furdina and J. Kossut, *Semiconductors and Semimetals*, ed. by R. K. Willardson and A. C. Beer, Academic, New York, Vol. **25** (1988). J. K. Furdina, J. Vac. Sci. Technol. A **4**, 2002 (1986).
2. J. Slinkman, A. Zhang, and R. E. Doezema, Phys. Rev. B **39**, 1251 (1990).
3. Y. Takada, K. Arai, and Y. Uemura, *Lecture Notes in Physics, Proc. of the Fourth International Conference on Physics of Narrow Gap Semiconductors, Linz, Austria* (1981), Vol. 125, Springer-Verlag, Berlin (1982), p. 101.
4. V. F. Radantsev, T. I. Deryabina, G. I. Kulaev et al., Phys. Rev. B **53**, 15756 (1996).
5. A. V. Germanenko, G. M. Min'kov, V. A. Larionova et al., Phys. Rev. B **54**, 1841 (1996).
6. G. Grabecki, T. Dietl, J. Kossut et al., Surf. Sci. **142**, 558 (1984).
7. G. Grabecki, T. Dietl, P. Sobkowicz et al., Appl. Phys. Lett. **45**, 1214 (1984).
8. T. Suski, P. Wisniewski, L. Dmowski et al., J. Appl. Phys. **65**, 1203 (1989).
9. G. Grabecki, A. Wittlin, T. Dietl et al., Semicond. Sci. Technol. **8**, S95 (1993).
10. P. Sobkowicz, G. Grabecki, T. Suski et al., Acta Phys. Pol. **A75**, 39 (1989).
11. V. F. Radantsev, T. I. Deryabina, L. P. Zverev et al., Zh. Eksp. Teor. Fiz. **88**, 2088 (1985).
12. Yu. A. Bychkov and E. I. Rashba, J. Phys. C. **17**, 6039 (1984).
13. V. F. Radantsev, Zh. Eksp. Teor. Fiz. **96**, 1793 (1989).
14. J. Luo, H. Munekata, F. F. Fang et al., Phys. Rev. B **41**, 7685 (1990).
15. B. Das, S. Datta, and R. Reifenberger, Phys. Rev. B **41**, 8278 (1990).
16. G. Engels, J. Lange, Th. Schapers et al., Phys. Rev. B **55**, R1958 (1997).
17. J. Nitta, T. Akazaki, H. Takayanagi et al., Phys. Rev. Lett. **78**, 1335 (1997).
18. J. P. Heida, B. J. van Wees, J. J. Kuipers et al., Phys. Rev. B **57**, 11911 (1998).
19. L. Wissinger, U. Rössler, R. Winkler, B. Jusserand, and D. Richards, Phys. Rev. B **58**, 15375 (1998).
20. V. F. Radantsev, Semicond. Sci. Technol. **8**, 394 (1993).
21. F. Stern and W. E. Howard, Phys. Rev. **163**, 816 (1967).

22. G. Bastard and C. J. Lewiner, *J. Phys. C* **13**, 1469 (1980).
23. D. Heiman, Y. Shapira, S. Foner et al., *Phys. Rev. B* **29**, 5634 (1984).
24. Ya. B. Zel'dovich and V. S. Popov, *Usp. Fiz. Nauk* **105**, 403 (1971).
25. A. B. Migdal, V. S. Popov, and D. N. Voskresenskii, *Zh. Eksp. Teor. Fiz.* **72**, 834 (1977); A. B. Migdal, *Fermions and Bosons in Strong Fields*, Moscow, Nauka (1978).
26. V. F. Radantsev, *Zh. Eksp. Teor. Fiz.* **115**, 1002 (1999).
27. N. J. Bassom and R. J. Nicholas, *Semicond. Sci. Technol.* **7**, 810 (1992).
28. L. P. Zverev, V. V. Kruzhaev, G. M. Min'kov et al., *Zh. Eksp. Teor. Fiz.* **86**, 1073 (1984).
29. L. P. Zverev, V. V. Kruzhaev, G. M. Min'kov et al., *Fiz. Tverd. Tela.* **26**, 2943 (1984).
30. J. Furdyna, *J. Appl. Phys.* **64**, R29 (1988).
31. I. A. Merkulov, D. R. Yakovlev, A. Keller et al., *Phys. Rev. Lett.* **83**, 1431 (1999).
32. A. K. Bhattacharjee, *Phys. Rev. B* **58**, 15660 (1998).
33. W. Dobrowolski, von M. Ortenberg, and A. M. Sandauer, *Lecture Notes in Physics, Proc. of the Fourth International Conference on Physics of Narrow Gap Semiconductors, Linz, Austria* (1981), Vol. **152**, Springer-Verlag, Berlin (1982), p. 302.
34. V. F. Radantsev, T. I. Deryabina, L. P. Zverev et al., *Zh. Eksp. Teor. Fiz.* **91**, 1016 (1986).